Cytokinesis in Tobacco BY-2 and Root Tip Cells: A New Model of Cell Plate Formation in Higher Plants

A. Lacey Samuels, Thomas H. Giddings, Jr., and L. Andrew Staehelin

Department of Molecular, Cellular, and Developmental Biology, University of Colorado, Boulder, Colorado 80309-0347

Abstract. Cell plate formation in tobacco root tips and synchronized dividing suspension cultured tobacco BY-2 cells was examined using cryofixation and immunocytochemical methods. Due to the much improved preservation of the cells, many new structural intermediates have been resolved, which has led to a new model of cell plate formation in higher plants. Our electron micrographs demonstrate that cell plate formation consists of the following stages: (*1*) the arrival of Golgi-derived vesicles in the equatorial plane, (*2*) the formation of thin (20 ± 6 nm) tubes that grow out of individual vesicles and fuse with others giving rise to a continuous, interwoven, tubulo-vesicular network, (*3*) the consolidation of the tubulo-vesicular network into an interwoven smooth tubular network rich in callose and then into a fenestrated plate-like structure, (*4*) the formation of hundreds of finger-like projections at the margins of the cell plate that fuse with the parent cell membrane, and (*5*) cell plate maturation that includes closing of the plate fenestrae and cellulose synthesis. Although this is a temporal chain of events, a developing cell plate may be simultaneously involved in all of these stages because cell plate formation starts in the cell center and then progresses centrifugally towards the cell periphery. The "leading edge" of the expanding cell plate is associated with the phragmoplast microtubule domain that becomes concentrically displaced during this process. Thus, cell plate formation can be summarized into two phases: first the formation of a membrane network in association with the phragmoplast microtubule domain; second, cell wall assembly within this network after displacement of the microtubules. The phragmoplast microtubules end in a filamentous matrix that encompasses the delicate tubulo-vesicular networks but not the tubular networks and fenestrated plates. Clathrin-coated buds/vesicles and multivesicular bodies are also typical features of the network stages of cell plate formation, suggesting that excess membrane material may be recycled in a selective manner. Immunolabeling data indicate that callose is the predominant lumenal component of forming cell plates and that it forms a coat-like structure on the membrane surface. We postulate that callose both helps to mechanically stabilize the early delicate membrane networks of forming cell plates, and to create a spreading force that widens the tubules and converts them into plate-like structures. Cellulose is first detected in the late smooth tubular network stage and its appearance seems to coincide with the flattening and stiffening of the cell plate.

CYTOKINESIS in higher plants is the process of partioning the cytoplasm by the formation of a new cell wall between daughter cells. This process is accomplished by the formation of the phragmoplast that not only builds the new plate but spatially orients it within the cell relative to the whole plant or organ axis. The phragmoplast of higher plant cells has been described as consisting of three main components: microtubules, microfilaments, and membranous elements (Schopfer and Hepler, 1991). While recent work has elucidated the roles and distributions of the cytoskeletal elements involved in cytokinesis (Baskin and Cande, 1990; Lambert, 1993; Yasuhara et al., 1993; Asada and Shiboaka, 1994), our knowledge of the membranous elements of the forming cell plate has not improved since the early descriptions of cell plate formation (Hepler and Newcomb, 1967; Cronshaw and Esau, 1968; Hepler and Jackson, 1968; Roberts and Northcote, 1970; Hepler, 1982; Gunning, 1982). These studies described the formation of the cell plate beginning in late anaphase, with an aggregation of Golgi-derived vesicles in the equatorial plane of the interzone between the separating chromatids. Fusion of vesicles produced membranous structures known as "bilobed bodies" and "branched bodies" (Hepler and Newcomb, 1967; Jones and Payne, 1978; Hepler, 1982) and at later stages, "islands of vesicular aggregates" (Cronshaw and Esau, 1968; Hepler and Bonsignore, 1990). These vesicular aggregates joined to produce a disk shaped new cell wall that ex-

Please address all correspondence to Dr. A. L. Samuels, Department of Botany, 3529-6270 University Blvd., Vancouver, B.C., Canada, V6T 1Z4. Tel.: (604) 822-6996. Fax: (604) 822-6089.

© The Rockefeller University Press, 0021-9525/95/09/1345/13 $2.00

panded centrifugally, after the centrifugal expansion of a cylinder of microtubules until it contacted the parent cell wall and joined (Schopfer and Hepler, 1991). As the new wall expanded, strands of endoplasmic reticulum traversing the wall were trapped; plasmodesmata formed at these sites (Hawes et al., 1981; Hepler, 1982).

While these descriptions are all consistent with one another, all of the samples were prepared using chemical fixatives that are known to act slowly and produce vesiculation of sensitive intracellular membranes (Mersey and McCully, 1978; Gilkey and Staehelin, 1986). Recent studies of cryofixed plant root tip cells (Kiss et al., 1990; Staehelin et al., 1990) have demonstrated the superiority of cryofixation techniques for studying dynamic and delicate membrane systems. The main advantage of cryofixation techniques is that all cellular components can be immobilized within milliseconds by solidifying cellular water (Jones, 1984; Dahl and Staehelin, 1989). Hyde et al. (1991) have already demonstrated the usefulness of cryofixation/freeze-substitution for studying cytokinesis in the multinucleate zoosporangium of the Oomycete *Phytophthora*.

The objective of this study was to reexamine the transient membrane conformations of the forming cell plate in cryofixed cells. Tobacco root tips and tobacco suspension cultured cells that had been induced to divide synchronously were high pressure frozen, and then subjected to freeze-substitution, or propane jet frozen and freeze fractured. Cell wall components, callose and cellulose, were localized using colloidal gold cytochemistry. Our electron micrographs provide a number of new insights into the morphological and chemical events associated with cytokinesis in higher plants, in which extensive membrane networks predominate and cell wall molecules such as callose and cellulose appear to play a significant role in the restructuring of these networks.

Materials and Methods

Cell Cultures and Synchronization of Mitosis

Tobacco *Nicotiana tabacum* Bright Yellow-2 (BY-2)[1] suspension cultured cells were grown in modified Linsmaier and Skoog medium and subcultured every 7 d (Nagata et al., 1992). Cell division was synchronized using the technique of Kakimoto and Shiboaka (1988). An aliquot of 5 ml of cell suspension, 5–8 d after subculturing, was added to 95 ml of medium containing 5 μg/ml aphidicolin (aphidicolin from Sigma) an inhibitor of DNA synthesis (aphidicolin was made up in a stock solution of 5 mg/ml in DMSO; we have subsequently found that aphidicolin from Calbiochem-Novabiochem (La Jolla, CA) or Fluka (Rokonkoma, NY) gave more consistent results and could be used at 3 μg/ml). After 24 h in aphidicolin-containing medium, the cells were placed in a reusable Nalgene filter holder fitted with a 30-μm nylon mesh and the aphidicolin washed out, with four washes of 250 ml of medium for 15 min each. After the washes, cells were resuspended in fresh medium and cultured for an additional 3 h, at which time 6 μM propyzamide (also known as pronamide, a microtubule assembly inhibitor) was added from a 10-mM stock solution in DMSO. The cells were cultured in the presence of propyzamide for an additional 6 h, and then the propyzamide washed out with three washes of 250 ml of medium for 10 min each. The mitotic index of the cell population was determined by fixing an aliquot of cells with 3:1 ethanol/acetic acid for at least 20 min, followed by a rinse in medium and staining with 1 μg/ml DAPI added from a stock solution of 0.5 mg/ml in acetone. Just before the propyzamide was washed out, the cells were arrested in prometaphase; the mitotic index ranged between 39–77%, with a mean of 55% for six experiments. Although the variability in the synchronization was high, it was a vast improvement over unsynchronized samples where the mitotic index ranged from 5–8%, with a mean of 7%. After propyzamide was washed out, the mitotic spindles reassembled and the cells proceeded through mitosis. It took about 90 min for the majority of cells to reach telophase; propane jet freezing or high pressure freezing was done from 90–150 min after propyzamide washout.

1. *Abbreviation used in this paper*: BY-2, bright yellow-2.

High Pressure Freezing and Freeze Substitution

Cells in telophase were suspended in a nonpenetrating cryoprotectant, 25% dextran (39,000 mol wt; wt/vol prepared in medium), and concentrated on a 30-μm nylon mesh. For high pressure freezing, an aliquot of cell slurry was transferred to gold sample holders that had been dipped in 100 mg/ml lecithin in chloroform and allowed to dry. The holder was immediately frozen in a Balzers HPM 010 high pressure freezer, and then quickly transferred to liquid nitrogen for storage. Sample holders were split open under liquid nitrogen and put into cryo-substitution vials containing 2% osmium tetroxide and 8% dimethoxypropane in anhydrous acetone. Substitution was carried out at −80°C for 2–3 d in a bath of acetone and dry ice, and then slowly warmed to −20°C for 2 h, 4°C for 2 h and room temperature for 2 h. After several rinses in acetone, the samples were teased from the sample holders with a fine needle. Infiltration was in epoxy resin (EMBED 812) according to the following schedule: 10% resin in acetone overnight; 25, 50, 75,and 100% (twice) 24 h, final embedding and thermal cure at 60°C.

Root tip samples were high pressure frozen and freeze substituted as described by Kiss et al. (1990). Seeds of *Nicotiana sylvestris* were germinated on vertically oriented nutrient agar plates. After 6 d, the distal 1-mm tips of the 4–7-mm roots were excised with a razor blade and immersed in 15–20% aqueous dextran, and then transferred to sample holders for high pressure freezing. Freeze-substitution followed the protocol used for BY-2 cells except that some samples were embedded in Spurr's resin. Root tip samples used for immunolabeling were freeze-substituted in 0.1% osmium in acetone and embedded in EMBED 812 resin.

Immunocytochemistry and Preparation of Cellobiohydrolase I–Gold Probe

Callose was localized using a monoclonal antibody to β-1,3-glucan from Biosupplies Australia, PtyLtd. (Parkville, Victoria, Australia). Sections from epoxy resin blocks were picked up on formvar coated nickel grids. The sections were floated on a 5-μl drop of saturated sodium metaperiodate for 10 min in a humid environment. All subsequent processing was carried out in 10 mM phosphate buffer with 0.25 M sodium chloride and 0.1% Tween-20 (PBST). Nonspecific protein binding was blocked by floating grids on drops of 5% (wt/vol) nonfat dried milk in PBST for 20 min. Primary antibody, diluted 1:50 in PBST plus 2.5% nonfat dried milk, was applied for 1 h at room temperature. Grids were rinsed with a stream of PBS supplemented with 0.5% Tween-20, and then transferred to secondary anti–mouse IgG conjugated to 15-nm colloidal gold that had been diluted 1:10 for 1 h. After another rinse in high Tween PBS, the grids were rinsed in warm distilled water and poststained as above. Binding of colloidal gold was abolished on sections incubated in buffer instead of primary antibody or antibodies preincubated with 1 mg/ml laminarin to block the epitope binding site.

Cellobiohydrolase I was the gift of Dr. M. Shulein (Novo Nodursk, Danbury, CT) and was conjugated to colloidal gold as described in Bonfante-Fasalo et al. (1990). 14-nm colloidal gold particles were produced by the reduction of chloroauric acid with sodium citrate (Hayat, 1991). After the pH was adjusted to 4.5 using HCl, 100 μl of 2 mg/ml cellobiohydrolase I was added to 10 ml of colloidal gold; after this conjugation, 500 μl of 1% PEG was added for added stability. The cellobiohydrolase I–gold was separated from unconjugated protein by centrifuging for 1 h at 12,100 *g*. The clear supernatant was discarded and the red pellet resuspended and recentrifuged. The final red pellet was carefully removed, leaving the blackish red residue of aggregated gold. The pellet was resuspended in citrate buffer, pH 4.5, with 0.1% PEG. To stain sections, high pressure frozen/freeze substituted samples that had been embedded in epoxy resin were incubated in sodium metaperiodate and nonfat dry milk as described above. Then the sections were floated on a drop of citrate buffer, pH 4.5, for 10 min. The cellobiohydrolase I–gold was centrifuged in a benchtop microfuge for 15 min before use to remove aggregates. The gold conjugate was diluted 1:20 in citrate buffer and the sections incubated for 20 min at room temperature. After rinsing in a stream of citrate buffer for 20 s, the

sections were rinsed in a stream of warm distilled water for 20 s and post-stained.

Sections (75–90 nm) were cut on a Reichert Ultracut E, picked up on formvar-coated copper grids and stained with 2% aqueous uranyl acetate for 20 min followed by Reynold's lead citrate for 5 min. Samples were viewed on a Zeiss EM10C or a JEOL 100 CX. Measurements were made using NIH Image version ppc 1.56 on images scanned into a Mac Power PC. All descriptive statistics are expressed as mean ± SD. As the frequency distributions of the data were normally distributed, comparisons of tubule diameters were made using Student's t test ($p = 0.01$).

Preparation of Freeze-Fracture Replicas

For freeze-fracture, cells were propane jet frozen with extracellular cryoprotectant (25% dextran, as described for high pressure freezing). Cells were concentrated on a 30-μm nylon mesh and picked up on a copper slot EM Grid. The grid was sandwiched between two copper replica supports and immediately inserted into the propane jet freezer. Jets of liquid propane cooled to at least −170°C were applied to both sides of the replica supports, which were then dropped into liquid nitrogen. Propane jet replica holders or high pressure freezing sample holders were transferred to the Balzers 360 freeze fracture unit, and then fractured and shadowed at −111°C. Replicas were cleaned by an overnight full strength bleach bath, followed by 45 min in 70% sulfuric acid at 60°C, and 2 h in 0.25 M chromic acid (Platt-Aloia and Thomson, 1982; Staehelin and Chapman, 1987). Suspension cultured cells tended to fracture through the plane of the parent plasma membrane, rather than through the cell plate or cytoplasm.

Results

Cell plate formation in plant cells is a multistep process that starts during late anaphase and is completed by late telophase. When visualized in ultrarapidly frozen tobacco cells, a series of well defined stages during cell plate development were observed. Although this is a temporal chain of events, a maturing cell plate may be simultaneously involved in nearly all of these stages because cell plate formation starts in the cell center and then progresses centrifugally towards the cell periphery. During this process, the "leading edge" of the expanding cell plate is associated with the phragmoplast microtubules that become concentrically displaced until they reach the parent cell plasma membrane.

The following description of cell plate formation is based on electron micrographs of both high pressure frozen and freeze-substituted tobacco root tips and synchronized dividing tobacco BY-2 suspension cultured cells. The same characteristic stages of cell plate development, described below, were observed in both experimental systems and no distinction between the cell types is made in the text except in the figure legends.

Membrane Events Associated with the Phragmoplast Microtubule Domain

In the earliest stages of cell plate formation, a cloud of vesicles is seen to gather in the equatorial plane of the interzone between the sister chromatids during late anaphase (Fig. 1). Although these vesicles are Golgi-derived, no Golgi stacks, nor other bulky organelles, such as plastids, are seen lodged between the tightly packed microtubules. Of the membranous organelles, only endoplasmic reticulum, multivesicular bodies, and occasionally small (0.2–0.5 μm) vacuoles appear in the zone of exclusion defined by the phragmoplast microtubules.

Fusion of the vesicles appears to start shortly after they reach the equatorial plane area and, as illustrated in the en face view of Fig. 2, involves unique fusion structures not previously reported in the literature. In particular, the in-

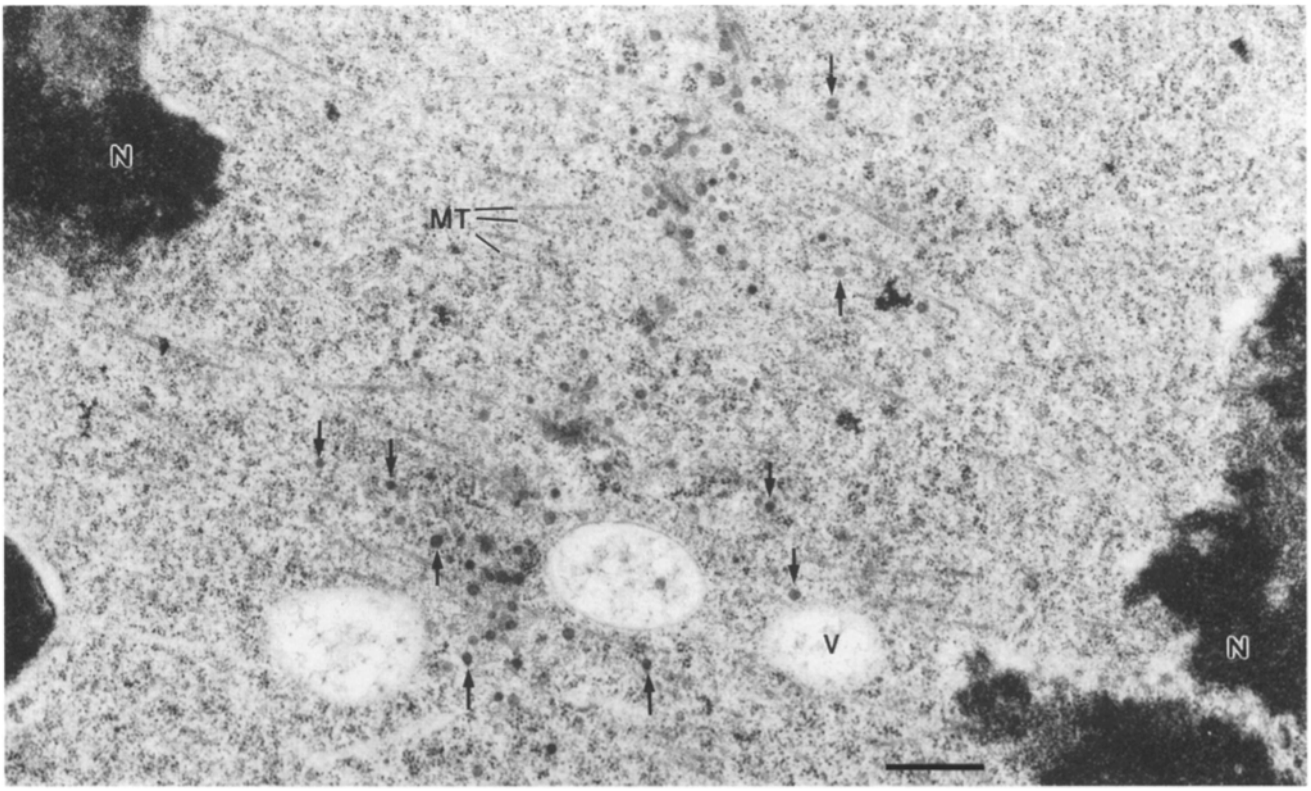

Figure 1. Overview of tobacco root tip cell in late anaphase, when cell plate vesicles (*arrows*) are beginning to arrive at the equator. (*N*, reforming nuclei; *V*, small vacuole; *MT*, microtubules). Bar, 0.5 μm.

dividual cell plate–forming vesicles, which are uniformly small in diameter (64 nm ± 12 nm; mean ± SD) exhibit long thin tubular extensions (20 nm ±6) that often appear coated with a fuzzy coat of undefined composition (Fig. 2, *b–d*). As shown in Fig. 2, *c* and *d*, tangential sections through these very early stage cell plates exhibit dumbbell-shaped vesicle-tubule-vesicle configurations, which may arise from fusion of a tubular membrane extension with a second vesicle. Numerous cross-sectioned microtubules are seen interspersed between the vesicles. Of hundreds of cell plates examined, we have encountered very few at the "cloud of vesicles" stage. To test whether this was a consequence of the timing of our cryofixation, cells were cryofixed at 70–90 min after propyzamide release when most of the cells in the sample were making the anaphase-telophase transition. The majority of the cells contained mitotic spindles or early tubulo-vesicular networks. Furthermore, once more than a few vesicles were gathered at the plate, the narrow fusogenic tubes could be detected on or between some of the vesicles, suggesting that the onset of formation of these tubules is rapid and quickly converts the central region of the cell plate to the tubulo-vesicular network stage.

Conversion of the Membrane Rich Tubulo-Vesicular Network into a Callose-Rich, Smooth Tubular Network

By the end of the vesicle fusion stage, most vesicles in the equatorial plane are linked up with each other in the form of a continuous, interwoven tubulo-vesicular network (Fig. 3). Microtubules are prominently associated with this stage of plate development (Fig. 3, *a* and *b*, and Fig. 4), but as the phragmoplast microtubules are displaced centrifugally, the cell plate changes from a tubulo-vesicular network (Figs. 3 and 4) into a more open, smooth tubular network (Fig. 5). Multivesicular bodies were found in close association with the cell plate in all network stages of plate development (Figs. 4, 5 *b*, 6 *a*, and 7 *b*).

Aside from its typical morphology, the tubulo-vesicular network is characterized by a high density of clathrin-coated buds/vesicles and converging microtubules (Fig. 3). The membrane tubules that interconnect the vesicular domains of the network and occasionally extend into the ad-

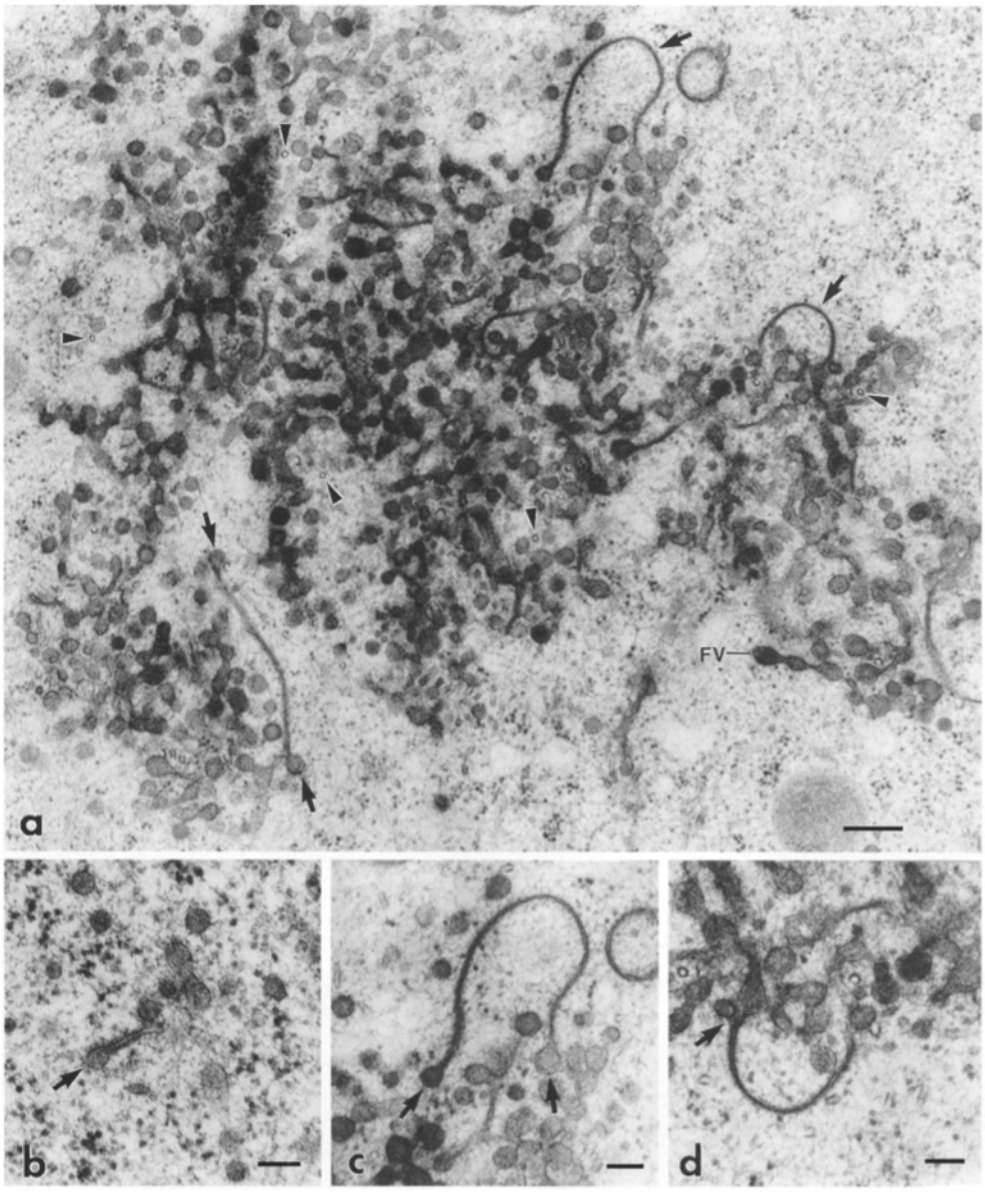

Figure 2. (*a*) En face view of the fusing cell plate vesicles (*FV*) of a tobacco BY-2 cell. Long thin membrane tubes (*arrows*) extend between vesicles; microtubules are interspersed among vesicles (*arrowheads*). Note that two structures marked by arrows are enlarged below in *c* and *d*. (*b*) Tube extending from a vesicle (*arrow*) during early cell plate formation (in root tip cell). The tube appears coated with a fuzzy coat of undetermined origin. (*c*) Typical vesicle-tubule-vesicle structures (*arrows*) that appear to arise from the fusion of a tube extending from one vesicle with an adjacent vesicle. (*d*) Earliest stages of a forming network; note the transition between the tubular and the tubulo-vesicular domains (*arrow*). Bars: (*b*) 100 nm; (*c*) 100 nm; (*c* and *d*) 0.25 μm; (*d*) 100 nm.

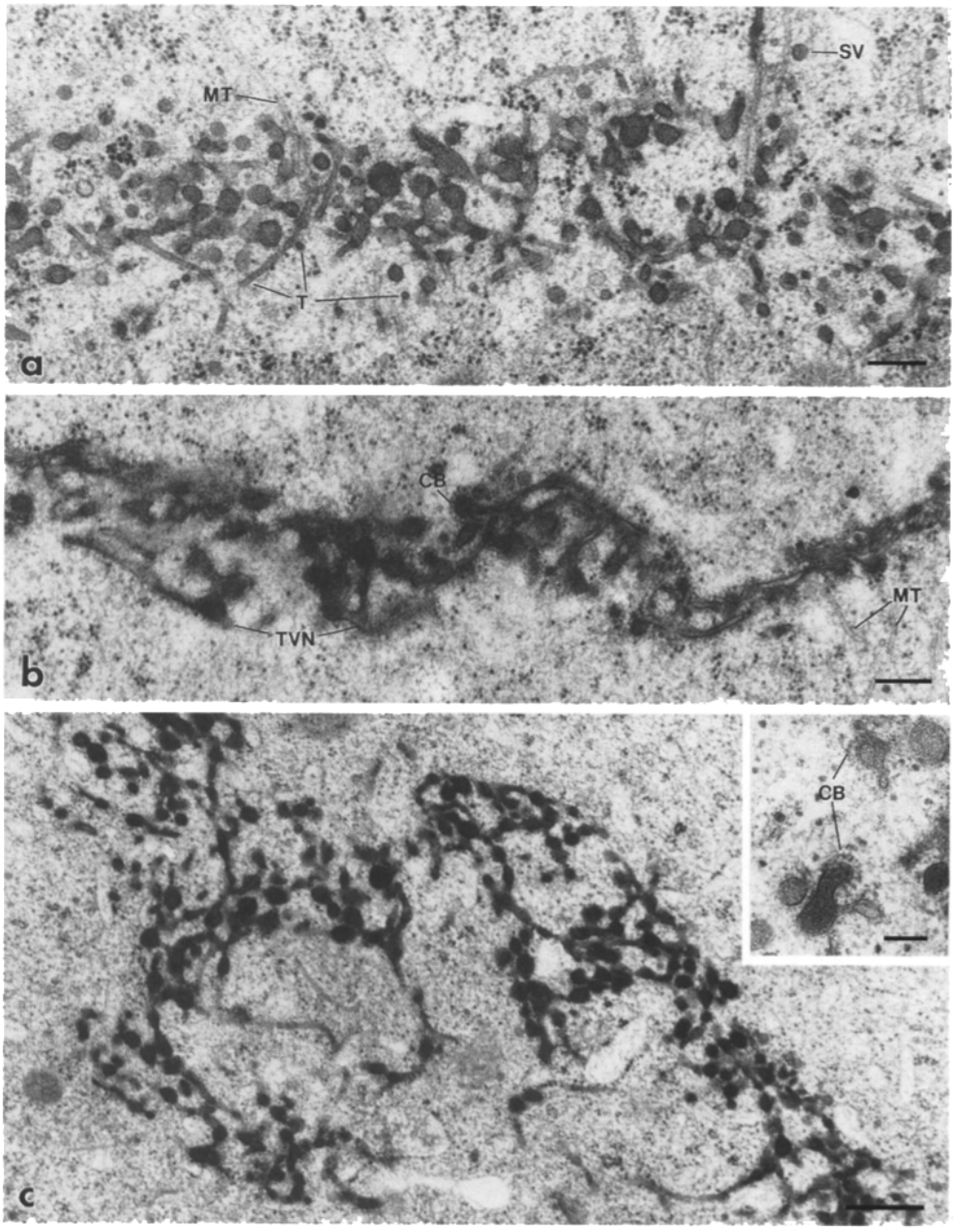

Figure 3. All micrographs of tobacco BY-2 cells. (*a*) Cross section through an early tubulo-vesicular network stage of cell plate formation. Abundant membrane tubes (*T*) extend into the adjacent cytoplasm that is rich in microtubules (*MT*). Secretory vesicles (*SV*) are seen associated with microtubules. (*b*) Cross section through a mature tubulo-vesicular network (*TVN*). Membranes of the network have a fuzzy, indistinct coat of unknown origin as well as spiky, clathrin buds (*CB*) and associated microtubules (*MT*). (*c*) Tangential section through a tubulo-vesicular network. This network is characterized by delicate membrane tubes extending between vesicular boli. (*c, inset*) High magnification of tubulo-vesicular network clathrin coats (*CB*) that are typical of this stage of cell plate development. Bars: (*a*) 0.25 μm; (*b*) 0.25 μm; (*c*) 0.5 μm; (*c, inset*) 100 nm.

jacent cytoplasm (Fig. 3, *a* and *c*), tend to have a constant diameter of 35 nm ± 6 nm; this is slightly but statistically significantly wider than the very thin tubules that appear between vesicles in the earliest stages of plate formation (Fig. 2). As illustrated in Fig. 3, clathrin-coated membranes are a common structural feature of the tubulo-vesicular network, and typically bud from vesicular rather than tubular portions of the network (Fig. 3, *b* and *c*). A relatively dense, fine filamentous, ribosome excluding matrix fills the spaces between the network elements and coats the membranes (Fig. 3 *b*); the phragmoplast microtubules also terminate in this matrix (Fig. 4).

The smooth tubular network arises from the tubulo-vesicular network after displacement of the phragmoplast microtubules and concurrently with the accumulation of new cell wall components in the lumen of the network (Figs. 4 and 5). The characteristic tubular elements of this network are smooth, extended, and loosely interwoven; there are large gaps of cytoplasm between the tubular elements (Fig. 5, *a* and *b*). This network labels strongly with anti–callose-gold complexes (Fig. 5 *a*). The nuclear envelope has reformed by this stage. The ovoid nuclei and large organelles have moved into the microtubule-free cytoplasm adjacent to the cell plate. Clathrin-coated buds/vesicles are commonly associated with this tubular network, but at a much lower frequency than the earlier, tubulo-vesicular network. This is the first stage of the forming cell plate that reacts with the cellulose binding probe, cellobiohydrolase I–gold; however, the reaction is weak compared to the parent wall suggesting the cellulose content of the cell plate at this stage is low (not shown).

Cell Plate Maturation, Fusion with the Plasma Membrane, and Completion of the New Cell Wall

The fusion of the cell plate with the plasma membrane co-

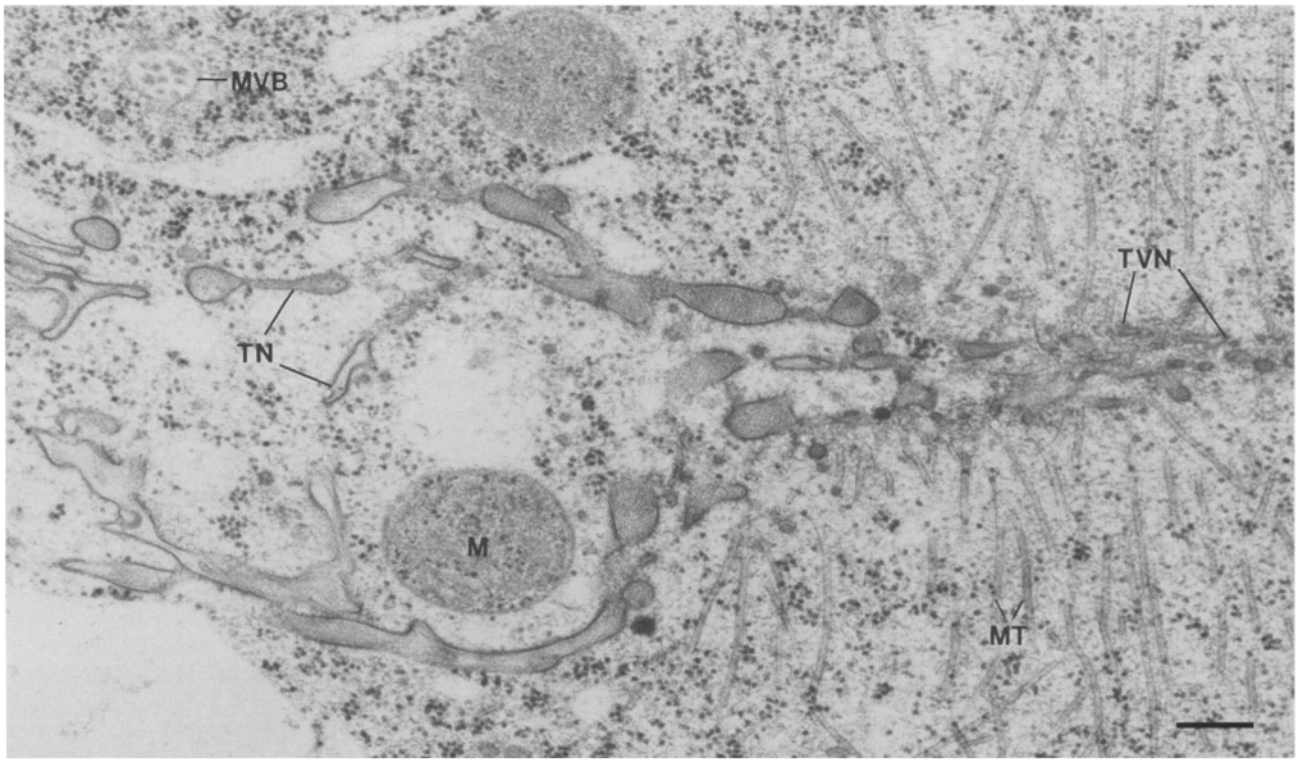

Figure 4. In this tobacco BY-2 cell, the section passed through the transition zone between the tubulo-vesicular network (*TVN*) and the tubular network (*TN*) domains of a forming cell plate. This transition zone, forms as the phragmoplast microtubules are displaced centrifugally and leave behind a network of phragmoplast membrane tubes (in this case towards the right). Network stages of cell plate development often have multivesicular bodies (*MVB*) in the adjacent cytoplasm. Note how the high density of phragmoplast microtubules (*MT*) associated with the tubulo-vesicular domain produces a "zone of exclusion," where bulky organelles are not found. (*M*, mitochondrion) Bar, 0.25 μm.

incides with the network consolidation phase of cell plate formation, i.e., with the formation of a fenestrated cell plate (Fig. 6). One of the most unexpected findings at this stage of cell plate formation is that fusion appears to be initiated nearly simultaneously at literally hundreds of sites by thin, finger-like projections that emanate from the margins of the forming cell plate (Fig. 7 *a*). These sites then expand to form a continuous transition between the new and old plasma membranes and cell walls (Fig. 7 *c*).

The flattening of the cell plate, which occurs after the cell plate margins link up with the parent plasma membrane (Gunning, 1982), appears to begin after the conversion of the tubular network (Fig. 5) into a fenestrated sheet (Fig. 6). This can be seen by comparing the waviness of the cross-sectional images of the forming cell plates in Figs. 3 and 5 with the flattened, fenestrated cell plate in Fig. 6 *b*. Also seen in Fig. 6 *b* are dense vesicles close to the cell plate whose staining pattern suggest that they may be delivering membrane and cell wall matrix materials to help close the last remaining cell plate fenestrae.

Plasmodesmata are rarely observed in suspension cultured tobacco BY-2 cells, thus it was difficult to observe their development in this study.

Kinetics of Deposition of Callose and Cellulose in Forming Cell Plates

Callose is first detected shortly after the initial vesicle fusion stage, and reaches maximum levels during the network consolidation phases including the tubular network and fenestrated plate stages (Figs. 5 *a*, 6 *b*, and 7 *b*). It is even found in the parent cell wall where the new plate attaches (Fig. 7 *b*), and finally disappears after all cell plate fenestrae have closed. Interestingly, as shown in Fig. 6 *b*, callose is more often detected near the surface of the plasma membrane rather than accumulating in the central layer of the forming cell plate, at least in the later stages of cell plate formation. Based on the amount of callose detected in this study, we estimate that even in the later stages of cell plate formation, callose is the predominant cell wall component found in the cell plate.

Cellulose appears to be a minor component of the cell plate; binding of the cellulose probe CBH I–gold to the plate is low compared to binding in the parent walls (Fig. 6 *c*). Cellulose is first detected in the tubular network and increases steadily through the fenestrated intermediates. Levels comparable to the parent wall are not reached until the plate has matured completely and abundant cortical microtubules are observed.

Discussion

Based on the improved morphological preservation of cryofixed, dividing tobacco cells used in this study, we propose a novel model of cell plate formation that consists of two principle phases: first, fusing Golgi-derived vesicles produce a membrane network dividing the cytoplasm; second, the new cell wall is assembled within this network. The stages that comprise these two processes are summarized diagrammatically in Fig. 8. The initial formation of the

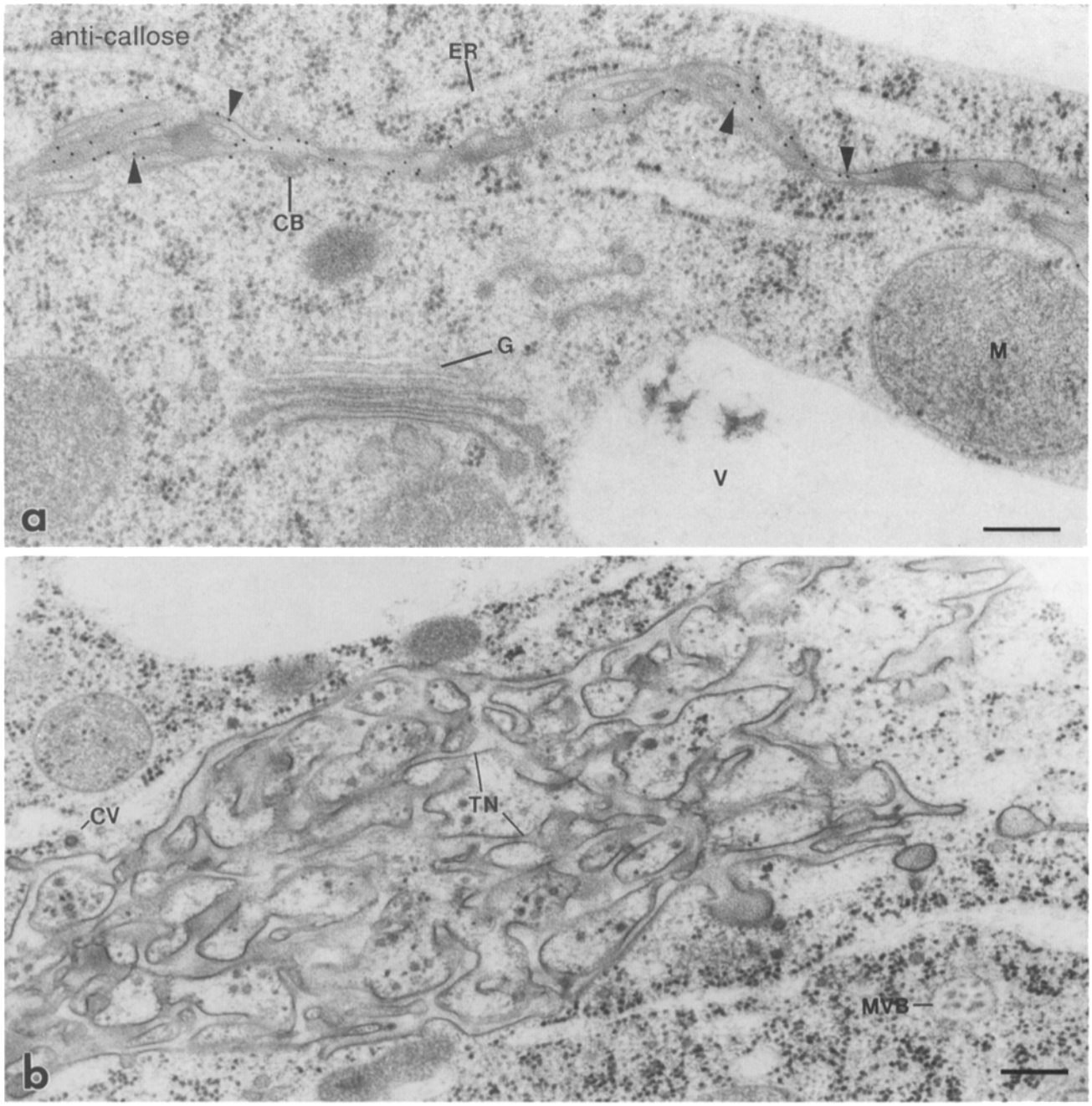

Figure 5. (*a*) Cross section of the tubular network stage of cell plate development in a tobacco BY-2 cell. Anti-callose antibodies label this stage heavily (e.g., *arrowheads*). A clathrin-coated vesicle is seen budding off the forming cell plate (*CB*). Bulky organelles such as plastids and Golgi (*G*) are seen in the vicinity of the plate. (*ER*, endoplasmic reticulum; *M*, mitochondrion). (*b*) Tangential section through a tobacco BY-2 cell plate at the tubular network stage (*TN*). The lumen of the network is more distended than during the previous stage and overall the network has a smoother outline (compare Fig. 3). Multivesicular body (*MVB*) and clathrin-coated vesicles (*CV*) are commonly observed. Bars: (*a*) 0.25 μm; (*b*) 0.25 μm.

membrane network includes rapid vesicle fusion and formation of the tubulo-vesicular network (Fig. 8, *a* and *b*). Our results indicate that the Golgi-derived vesicles do not simply "accumulate" upon arrival at the equatorial plane but instead quickly begin to fuse with each other to initiate the formation of the tubulo-vesicular network. Even as the fusion process begins, additional vesicles arrive and are incorporated into the network. The incorporation is most active at the periphery, resulting in the centrifugal expansion of the forming network.

The second phase of cell plate formation, the assembly of a new cell wall within the cell plate, begins with the consolidation of the tubulo-vesicular network into a smooth tubular network rich in callose (Fig. 8 *c*). Further expansion of the tubular elements appears to be driven primarily by polysaccharide assembly, resulting in the transformation of the smooth tubular network into a fenestrated, plate-like structure (Fig. 8 *d*). At the periphery of the fenestrated plate, tubular elements of the network extend outward forming large numbers of finger-like projections

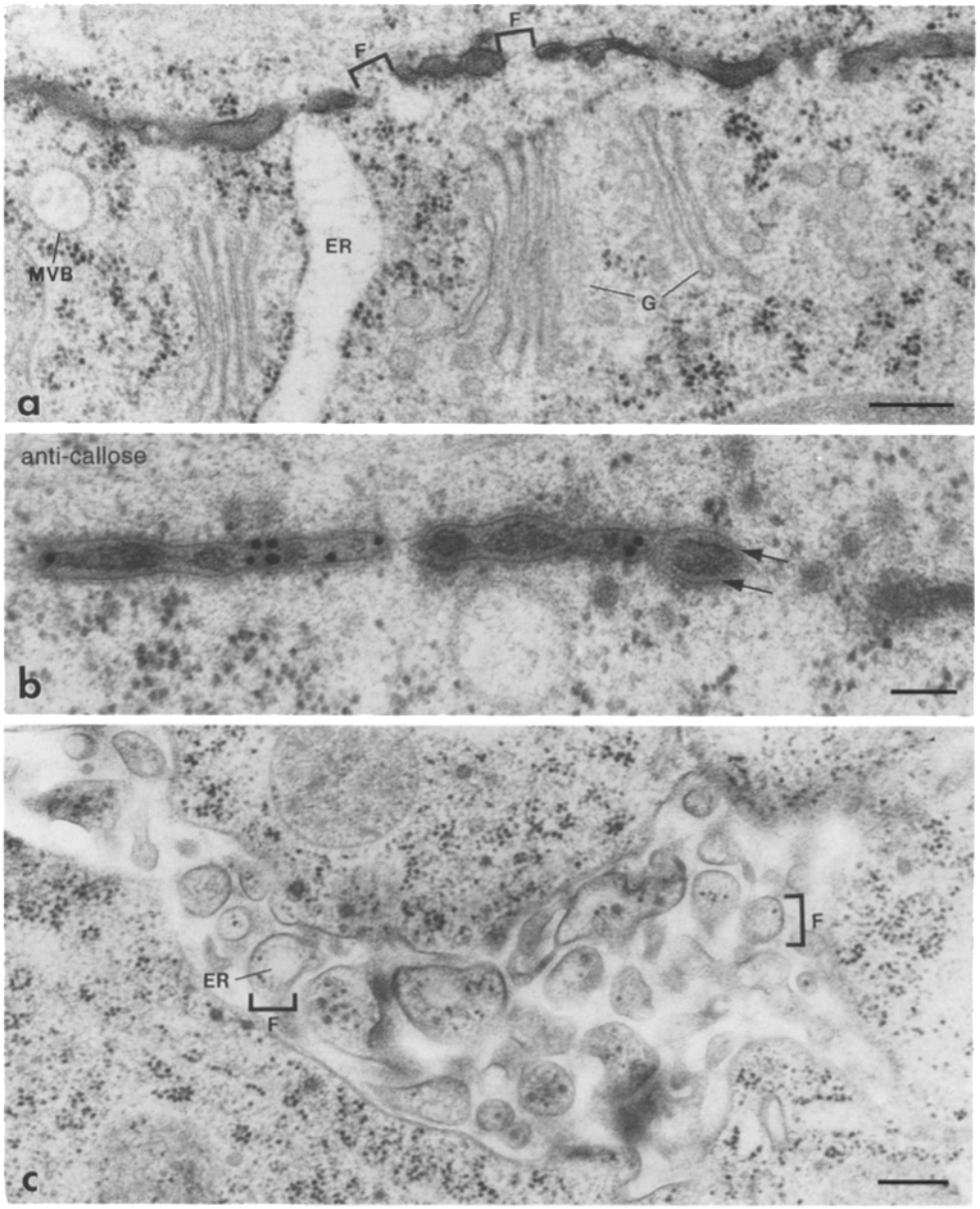

Figure 6. (*a*) Fenestrated plate stage of development in a tobacco BY-2 cell. Strands of endoplasmic reticulum (*ER*) traverse the plate through the fenestrae (*F*). Golgi stacks (*G*) are adjacent to the forming cell plate. (*MVB*, multivesicular body). (*b*) High magnification of a cell plate from a tobacco root tip that was labeled with anti-callose gold. Note that the gold particles are associated mostly with the lighter staining regions adjacent to the plasma membrane suggesting that the callose deposits are coating the membrane surface (*arrows*). (*c*) Tangential section through a fenestrated plate stage of a tobacco BY-2 cell. Within the fenestrae (*F*), strands of endoplasmic reticulum (*ER*) are seen surrounded by cytoplasm. (*a*) 0.25 μm; (*b*) 100 nm; (*c*) 0.25 μm.

that eventually reach and fuse with the parent cell plasma membrane (Fig. 8 *e*). This model has some features in common with earlier models, e.g., Gunning (1982): the plate forms from Golgi-derived vesicles, there is centrifugal expansion and there is a fenestrated plate intermediate. However, there are several important novel features such as rapid tubule formation and the formation of the tubulo-vesicular network, the callose rich smooth tubular network, and the finger-like projections that contact the parent cell wall.

Comparison of Cell Plate Images Produced by Cryo-Fixation and Conventional Chemical Fixation Techniques

The current view of cytokinesis in higher plants, based on conventional chemical fixation, is that the cell plate forms as the fusion product of long rows of vesicles (Hepler and Jackson, 1968; Yasuhara et al., 1993). In ultrarapidly frozen material, long files of vesicles were not observed; the vesicles were restricted to the earliest stages of plate development and around the periphery of the developing cell plate. The vesicles observed were exclusively of small (64 nm) diameter, rather than displaying a smaller size in the earlier stages of plate development and a mixture of small- and larger-sized vesicles during the later stages (Cronshaw and Esau, 1968; Hepler and Newcomb, 1967; Roberts and Northcote, 1970). The previously reported lines of vesicles probably resulted from the glutaraldehyde induced vesiculation of the networks observed in this study. The "branched" and "stellate" bodies between vesicles (Hepler and Newcomb, 1967; Jones and Payne, 1978; Hepler, 1982; Gunning, 1982) would correspond to remnants of the microtubule associated, tubulo-vesicular network described. In animal systems, endosomes have been shown to be tubulo-vesicular in living cells but fragmented in chemically fixed samples (Hopkins et al., 1990). The later stages of cell plate formation (late tubular and fenes-

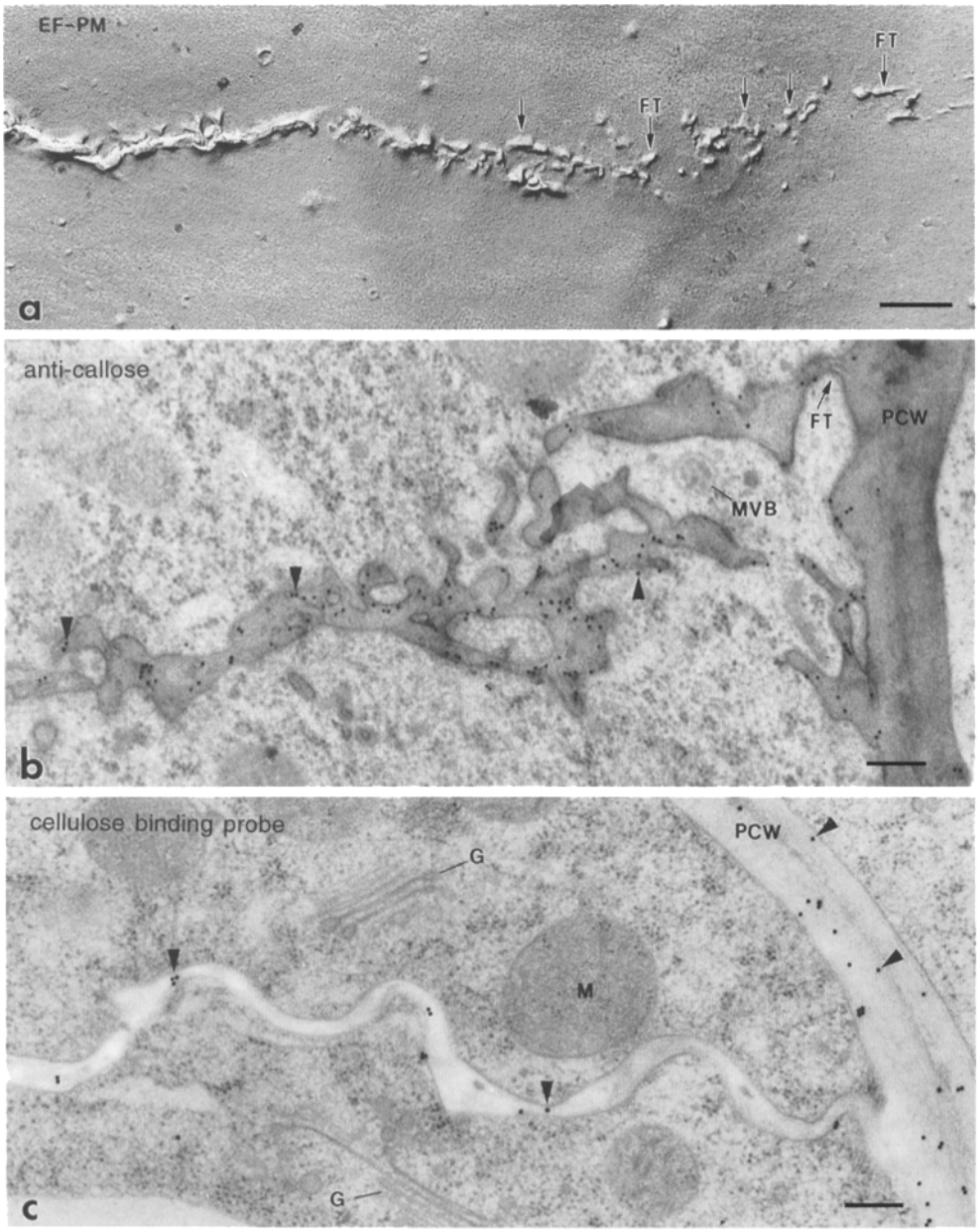

Figure 7. (*a*) Freeze fracture micrograph depicting the E-fracture face of the tobacco BY-2 cell parent plasma membrane (EF-PM) in the adhesion zone (see Fig. 8 *d*) where the cell plate is in the process of joining with the plasma membrane. The cell plate appears to be fusing with the parent membrane by a series of finger-like projections (*FT*, fused tubes, *arrows*) that gradually merge to incorporate the new cell wall and plasma membranes. (*b*) Cross-section of the cell plate of a tobacco BY-2 cell, joining with the parent cell wall (*PCW*). Heavy labeling with the anti–callose-gold is seen over the cell plate and over parts of the parent cell wall close to the sites of fusion between the cell plate and the parent plasma membrane (*arrowheads*). (*MVB*, multivesicular body). (*c*) Late fenestrated plate stage of cytokinesis in a tobacco BY-2 cell. The developing plate has joined with the parent cell wall (*PCW*) but still has a wavy conformation. Section labeled with cellobiohydrolase I-gold, a cellulose-binding probe (*arrowheads*). The parent cell wall is more heavily labeled than the cell plate, indicating the cellulose content of the cell plate was still quite low at the time of cryofixation. Note the angularity of the new plasma membrane as certain domains of the cell plate straighten. (G, Golgi stack; M, mitochondrion). Bars: (*a*) 100 nm; (*b*) 0.25 μm; (*c*) 0.25 μm.

trated sheets structures) appear to be somewhat better preserved in chemically fixed cells (Cronshaw and Esau, 1968; Jones and Payne, 1978), presumably due to the mechanical stabilization imparted by the assembling cell wall molecules. In addition to the artifactual vesiculation, the time it takes a chemical fixative to work may be long relative to the process being studied. Chemical fixatives have been estimated to take 10–30 s (Bajer and Mole-Bajer, 1971) to 15 min (Mersey and McCully, 1978) to immobilize cytoplasmic streaming in plant cells. All of the stages of cell plate formation shown in this study occur over a period of 40 min in tobacco BY-2 cells (Yasuhara et al., 1993), thus it is possible that during chemical fixation, significant rearrangements of cell plate components may take place during the time it takes for a chemical cross-linker to immobilize intracellular structures. In ultra-rapidly frozen/freeze substituted dividing plant cells, certain organelles are prominent, such as Golgi vesicles, the cell plate, and microtubules. However, other organelles such as endoplasmic reticulum and microfilaments were not as apparent. Conventional preparations, unless the endoplasmic reticulum was especially contrasted with zinc-iodide-osmium (Hawes et al., 1981; Hepler, 1982), have also suffered from this difficulty.

Fusion of the Cell Plate Vesicles

Two of the most striking novel features discovered in this study are the vesicle fusion tubules and the tubular nature of the earliest stages of plate formation. Recently, new theories have emerged that propose that tubule formation is a basic property of certain endomembranes such as the Golgi apparatus and endosomes (Hopkins et al., 1990; Cluett et al., 1993; Ayala, 1994). Most of these studies have emphasized the dynamic balance between tubulation and coat protein-driven vesiculation (Klausner et al., 1992),

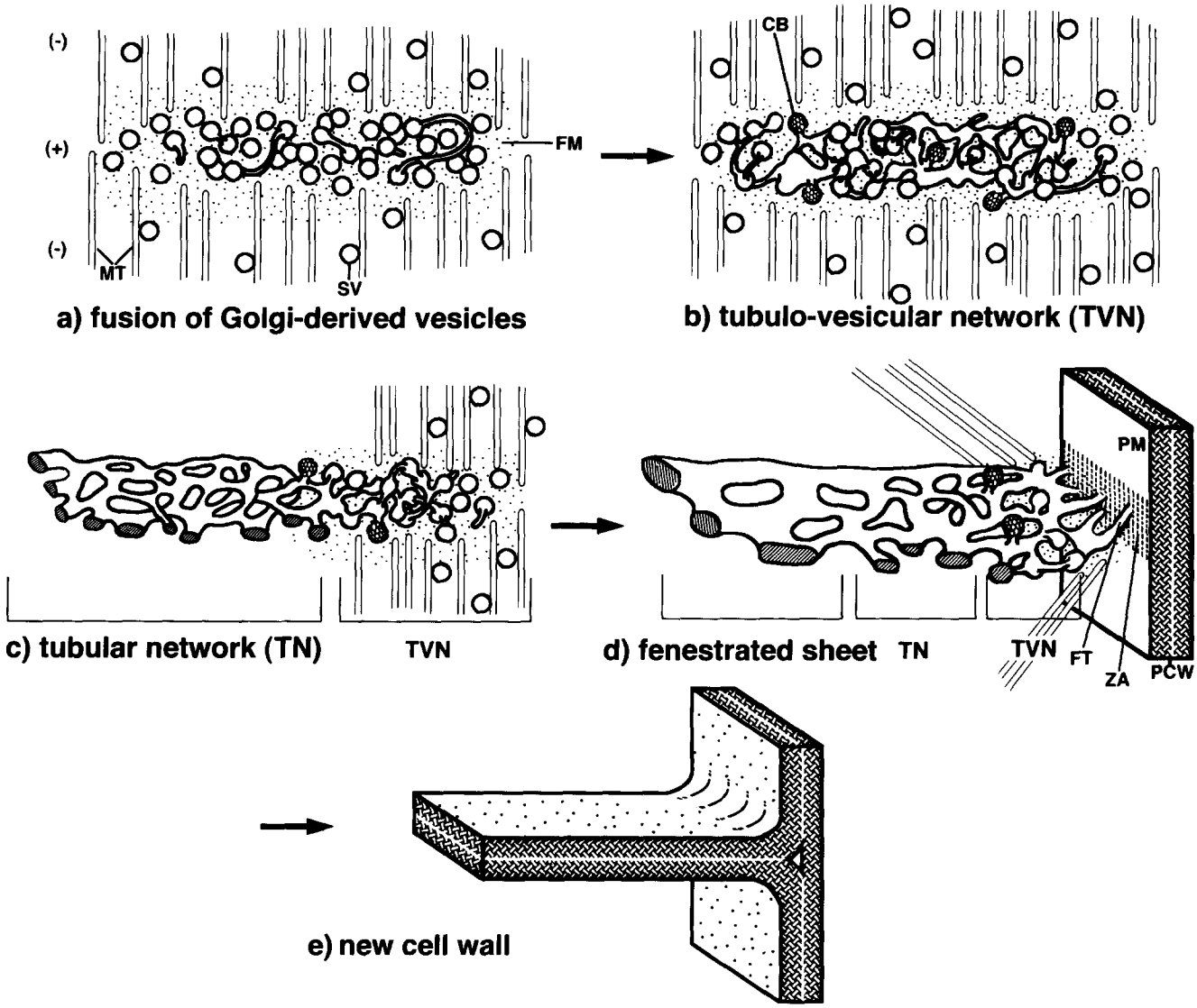

Figure 8. Model of cell plate development in a higher plant cell. (*a*) The fusion of Golgi-derived vesicles begins rapidly with the arrival of the secretory vesicles (*SV*) at the equatorial zone, amongst the phragmoplast microtubules (*MT*) and a cytoplasmic fuzzy matrix (*FM*). (*b*) A delicate tubulo-vesicular network is quickly formed from the fusing vesicles. Vesicular boli are interconnected by membrane tubules and clathrin-coated membrane buds (*CB*) are abundant. The phragmoplast microtubules are at a high density on this domain of the forming cell plate and the microtubules terminate in the fuzzy matrix surrounding the network. (*c*) The tubular network forms as the lumen of the tubulo-vesicular network (*TVN*) becomes filled with cell wall polysaccharides, especially callose. Besides a more extended smooth morphology, this stage is distinguished from the tubulo-vesicular network by the low density of microtubules present and less clathrin buds as well as high callose content. (*d*) As the cell wall is further assembled within the lumen of the membrane networks, the tubule areas are expanded and an almost continuous sheet forms. The fenestrae that are left open often contain strands of endoplasmic reticulum and in these sites plasmodesmata can form. The cell plate joins with the parent cell wall (*PCW*) by hundreds of finger-like fusion tubes (*FT*). The fusion tubes contact at the zone of adhesion (*ZA*) on the plasma membrane (*PM*) in the area formerly occupied by the preprophase band. The abundant microtubules present together with the tubulo-vesicular morphology of this area of the cell plate make it equivalent to the tubulo-vesicular network shown in *b*. (*e*) The new cell wall is smoothly coated by the plasma membranes. It is not until this stage that the cellulose content of the new cell wall becomes comparable to the parent cell walls.

but in this case tubules may be exclusively involved in membrane fusion and network formation rather than vesicle production. A 20-nm tubule has a high radius of curvature that has been postulated to reduce electrostatic repulsion and thereby aid membrane fusion (Poste and Allison, 1973). A similar type of tubule has been observed extending from "pyriformis" secretory vesicles in ultrarapidly frozen legume root hairs (Ridge, 1988). Jones and Payne (1978), in their classic study of cell plate formation in *Impatiens*, have previously suggested that "membranous arms" may aid vesicle fusion.

How the thin tubes that appear to mediate membrane fusion are made is not known. However, the recent demonstration that GTP-γS–induced assembly of dynamin rings in nerve terminals can lead to the formation of narrow (25–30 nm) tubes of uniform diameter (Takei et al., 1995), suggests a possible mechanism for the formation of the fusion tubes observed in this study. As seen in Fig. 2, *b*,

c, and *d*, fusion tubes of cell plate–forming vesicles do seem to carry a surface coat on their cytoplasmic surface, but the composition of this coat has yet to be determined.

Recycling of Membrane from the Network Phases of the Developing Cell Plate

The formation of a new cell wall between daughter cells requires mobilization of large amounts of membrane and secretory products from the ER-Golgi membrane systems. Without quantitative knowledge of how much of the cell plate consists of products such as cellulose and callose that are synthesized at the plasma membrane, it is difficult to estimate exactly how much excess plasma membrane is delivered to the cell plate by the secretory vesicles transporting wall materials. If the surface area of the secretory vesicles is greater than the surface area of the new plasma membranes, then some mechanism for membrane recycling must exist. The abundance of clathrin-coated buds/vesicles and multivesicular bodies associated with all network stages of cell plate formation would be consistent with the hypothesis that clathrin-coated vesicles play a major role in membrane recycling from the cell plate. In mammalian systems, the pinching off of clathrin-coated vesicles has been shown to be mediated by the protein dynamin (Damke et al., 1994; Hinshaw and Schmid, 1995); the forming cell plate with its high concentration of clathrin-coated vesicle budding may represent an excellent model system for testing the involvement of dynamin in vesicle fission reactions in plants.

Clathrin-coated vesicles have been shown to be involved in both receptor-mediated endocytosis (Pearse and Robinson, 1990) and in the sorting and packaging of vacuolar and lysosomal proteins in the *trans*-Golgi network (Hinz et al., 1993). In both instances, the role of the clathrin-coated vesicles is to selectively concentrate some types of molecules while excluding others. The fact that the clathrin-coated vesicles are involved in removing excess membrane from the forming cell plates suggests that this membrane recycling is not a random process but involves the selective removal of membrane components that are no longer needed. The appearance of multivesicular bodies adjacent to the cell plates suggests that many of these membrane proteins may be destined for lysosomal degradation; multivesicular bodies in mammalian systems are believed to be a class of endosomes containing membrane receptors destined for lysosomal breakdown (Felder et al., 1990).

Relationship between the Phragmoplast Cytoskeleton and the Cell Plate Membrane Networks

The presence of a dense matrix surrounding the tubulo-vesicular network provides a physical connection between the cytoskeleton and the membranes of the forming plate. In this study, the phragmoplast microtubules were observed terminating in this matrix; hook decoration assays have demonstrated that these are the plus ends of the phragmoplast microtubules (Euteneuer et al., 1982). This has been confirmed using immunofluorescence (Vantard et al., 1990; Asada et al., 1991) and fluorescent analog labeling (Zhang et al., 1990). Lambert (1993) has suggested that microtubules radiating from a nuclear envelope microtubule organizing center may be stabilized at the cell plate. The components of the dense matrix observed here could be involved in this stabilization.

The physical association between the phragmoplast microtubules and Golgi-derived vesicles (Figs. 1, 2, and 3 *a*; Gunning, 1982; Kakimoto and Shiboaka, 1988) is suggestive of a functional role for microtubules in transport of vesicles to the forming cell plate. Consistent with this idea, treatment of tobacco BY-2 cells with taxol, a microtubule stabilizing drug, leads to the continuous accumulation of vesicles at the cell plate (Yasuhara et al., 1993). Asada and Shiboaka (1994) have recently isolated a 125-kD protein from phragmoplasts, which, after experimental activation, causes translocation of microtubules in a minus-end direction. Because this same activity would induce microtubule-associated vesicles to be translocated towards the plus (equatorial) end of the microtubules, the 125-kD protein is an attractive candidate for bringing secretory vesicles to the cell plate.

Microfilaments, which colocalize with microtubules in the phragmoplast, are also possible cytoskeletal candidates for vesicle transport to the forming cell plate (for reviews see Baskin and Cande, 1990; Zhang et al., 1993). The orientation of the microfilaments in the phragmoplast is analogous to the orientation of the microfilaments that support transport of organelles during cytoplasmic streaming (Kakimoto and Shiboaka, 1988). However, when microfilaments are disrupted with cytochalasins, the cell plate still forms (unpublished observations; Palevitz, 1980), suggesting that vesicle delivery is not solely dependent on microfilament integrity.

The Roles of Callose and Cellulose in Cell Plate Assembly

The completion of the tubulo-vesicular network signals the end of the first stage of cell plate formation, the accumulation and fusion of Golgi-derived vesicles into a continuous network system, which defines where the new cell wall will be assembled. The cell wall assembly phase starts with the disappearance of the phragmoplast microtubules and the conversion of the tubulo-vesicular network into the tubular network. Based on our electron micrographs, and the following considerations, the maturation of the tubular network into a fenestrated cell plate and then into a cell wall may be driven primarily by the synthesis of callose, and the assembly of cell wall matrix polysaccharides with cellulose fibrils. Membrane network formation appears to trigger callose synthesis in the cell plate, since callose is never observed in the Golgi stacks or secretory vesicles (Fig. 5 *a*). The actual triggering event is most likely the rise in cytoplasmic calcium concentration. The phragmoplast-associated callose synthase enzyme complex requires the presence of calcium (Kakimoto and Shiboaka, 1992) and the presence of high calcium conditions at the forming cell plate have been demonstrated (Wolniak et al., 1980).

Callose has been repeatedly demonstrated in cell plates in the past (for reviews see Gunning, 1982; Kakimoto and Shiboaka, 1992). However, there was some concern that callose could be synthesized as the result of a fixation induced artifact. Callose synthesis is highly dependent on local calcium concentration (Kakimoto and Shiboaka, 1992;

Delmer, 1987) and chemical fixation destroys membrane integrity, causing cytoplasmic calcium concentration to increase. By avoiding exposing cells to chemical fixatives before ultra-rapid freezing, we have been able to eliminate this possibility. Significant labeling with the monoclonal antibody against callose was observed in our cryofixed samples, thus providing conclusive evidence for callose being a major component of normal cell plates.

The finding that even in later stages of cell plate assembly, callose is the predominant cell wall polysaccharide present in the cell plate suggests that callose may serve a critical function in cell plate assembly. What might this role be? Callose accumulation starts during the tubulovesicular phase of cell plate formation, but is most prominent during the conversion of the tubular network to the fenestrated sheet. Since callose is formed by enzymes located in the forming plasma membrane and appears to be deposited in a thick, coat-like layer over the membrane surface (Fig. 6 *b*), it may exert a spreading type of force on the membranes, which would facilitate widening of the tubules and their conversion to the plate-like components of the fenestrated sheet. In addition, the callose coat may provide mechanical support to the delicate tubular membrane network of the forming cell plate until the plate contains reinforcing assemblies of cell wall molecules. It has long been reported that cell plates exhibit a "quivering" motion before linking up with the plasma membrane (Gunning, 1982); this motion may reflect the jelly-like properties of the membrane-associated callose deposits of such cell plates.

In our study, the cell plate began to lose its wavy appearance when it reached the fenestrated sheet stage of development. It is interesting that at this stage, cellulose was beginning to be synthesized in significant amounts. It has been suggested that stiffening might occur as the ratio of microfibrils to matrix molecules increased (Gunning, 1982). Our immunolabeling results, showing abundant callose in the earlier, "wavy" stages and increasing cellulose coinciding with stiffness (Fig. 7 *c*), support this hypothesis. Cell wall matrix components (pectins and xyloglucans) can be immunolocalized in forming cell plates starting with the tubulo-vesicular stage, but the concentration only seemed to increase substantially after completion of the new cell wall (unpublished data and Moore and Staehelin, 1988).

Conclusions

Cell plate formation in higher plants commences with the fusion of vesicles into delicate membrane networks that are sensitive to conventional chemical fixation techniques and therefore have not been adequately visualized in the past. Based on our observations of cryofixed tobacco cells, the stages of cell plate development can be summarized (as illustrated in Fig. 8): (*1*) the arrival of Golgi-derived vesicles between the phragmoplast microtubules in the equatorial plane, (*2*) the formation of thin tubes that extend from individual vesicles and fuse with others giving rise to a tubulo-vesicular network, (*3*) the consolidation of the tubulo-vesicular network into a smooth tubular network, rich in callose and then into a fenestrated, plate-like structure, and (*4*) the formation of finger-like projections at the margin of the cell plate that fuse with the parent cell plasma membrane and (*5*) closing of the plate fenestrae.

The kind donation of cellobiohydrolase I by Dr. M. Shulein (Novo Nordusk, Danbury, CT) is gratefully acknowledged. T. Bier contributed experimental data to this project as part of an undergraduate independent study project. Thanks to M. Weis and E. Humphreys at the University of British Columbia Electron Microscopy Facility, and J. D'Antonio, H. Chial, and J. Meehl at the University of Colorado for help with synchronizations.

This work was supported by National Institutes of Health grant 18639 to L. A. Staehelin and a Canadian National Sciences and Engineering Council Postdoctoral Fellowship to A. L. Samuels.

Received for publication 6 March 1995 and in revised form 2 June 1995.

References

Asada, T., and H. Shibaoka. 1994. Isolation of polypeptides with microtubule-translocating activity from phragmoplasts of tobacco BY-2 cells. *J. Cell Sci.* 107:2249–2257.

Asada, T., S. Sonobe, and H. Shibaoka. 1991. Microtubule translocation in the cytokinetic apparatus of cultured tobacco cells. *Nature (Lond.).* 350:238–241.

Ayala, S.-J. 1994. Transport and internal organization of membranes: vesicles, membrane networks and GTP-binding proteins. *J. Cell Sci.* 107:753–763.

Baskin, T. I., and W. Z. Cande. 1990. The structure and function of the mitotic spindle in flowering plants. *Ann. Rev. Plant Phys.* 41:277–315.

Bajer, A., and J. Mole-Bajer. 1971. Architecture and function of the mitotic spindle. *Adv. Cell Mol. Biol.* 1:213–266.

Bonfante-Fasolo, P., B. Vian, S. Perotto, A. Faccio, and J. P. Knox. 1990. Cellulose and pectin localization in roots of mycorhizal *Allium porrum:* labeling continuity between host cell wall and interfacial material. *Planta.* 180:537–547.

Cluett, E. B., S. A. Wood, M. Banta, and W. J. Brown. 1993. Tubulation of Golgi membranes in vivo and in vitro in the absence of Brefeldin A. *J. Cell Biol.* 120:15–24.

Cronshaw, J., and K. Esau. 1968. Cell division in leaves of *Nicotiana. Protoplasma.* 65:1–24.

Dahl, R., and L. A. Staehelin. 1989. High pressure freezing for the preservation of biological structure: theory and practice. *J.E.M. Tech.* 13:165–174.

Damke, H., T. Baba, D. E. Warnock, and S. L. Schmid. 1994. Induction of mutant dynamin specifically blocks endocytic coated vesicle formation. *J. Cell Biol.* 127:915–934.

Delmer, D. P. 1987. Cellulose biosynthesis. *Ann. Rev. Plant Phys.* 38:259–290.

Euteneuer, U., W. T. Jackson, and J. R. McIntosh. 1982. Polarity of spindle microtubules in *Haemanthus* endosperm. *J. Cell Biol.* 94:644–653.

Felder, S., K. Miller, G. Moehren, A. Ullrich, J. Schlessinger, and C. R. Hopkins. 1990. Kinase activity controls the sorting of the epidermal growth factor receptor within the multivesicular body. *Cell.* 61:623–634.

Gilkey, J. C., and L. A. Staehelin. 1986. Advances in ultrarapid freezing for the preservation of cellular ultrastructure. *J.E.M. Tech.* 3:177–210.

Gunning, B. E. S. 1982. The cytokinetic apparatus: its development and spatial regulation. *In* The Cytoskeleton In Plant Growth and Development. C. W. Lloyd, editor. Academic Press, London. pp. 229–292.

Hawes, C. R., B. E. Juniper, and J. C. Horne. 1981. Low and high voltage electron microscopy of mitosis and cytokinesis in maize roots. *Planta.* 152:397–407.

Hayat, M. A. 1991. Colloidal Gold: Principles, Methods, and Applications. Academic Press, Inc., San Diego, CA. pp. 538.

Hepler, P. K. 1982. Endoplasmic reticulum in the formation of the cell plate and plasmodesmata. *Protoplasma.* 111:121–133.

Hepler, P. K., and E. H. Newcomb. 1967. Fine structure of cell plate formation in the apical meristem of Phaseolus roots. *J. Ultrastruc. Res.* 19:498–513.

Hepler, P. K., and W. T. Jackson. 1968. Microtubules and early stages of cell plate formation in the endosperm of *Haemanthus katherinea* Baker. *J. Cell Biol.* 38:437–446.

Hepler, P. K., and C. L. Bonsignore. 1990. Caffeine inhibition of cytokinesis: ultrastructure of cell plate formation/degradation. *Protoplasma.* 157:182–192.

Hinshaw, J. E., and S. L. Schmid. 1995. Dynamin self-assembles into rings suggesting a mechanism for coated vesicle budding. *Nature (Lond.).* 374:190–192.

Hinz, G., B. Hoh, and D. G. Robinson. 1993. Strategies in the recognition and isolation of storage protein receptors. *J. Exp. Bot.* 44:351–357.

Hopkins, C. R., A. Gibson, M. Shipman, and K. Miller. 1990. Movement of internalized ligand-receptor complexes along a continuous endosomal reticulum. *Nature (Lond.).* 346:335–339.

Hyde, G. J., S. Lancelle, P. K. Hepler, and A. R. Hardham. 1991. Freeze substitution reveals a new model for sporangial cleavage in *Phytophora,* a result with implications for cytokinesis in other eukaryotes. *J. Cell Sci.* 100:735–746.

Jones, G. J. 1984. On estimating freezing times during tissue rapid freezing. *J. Microsc.* 136:349–360.

Jones, M. G. K., and H. L. Payne. 1978. Cytokinesis in *Impatiens balsamina* and the effect of caffeine. *Cytobios.* 20:79–91.

Kakimoto, T., and H. Shibaoka. 1988. Cytoskeletal ultrastructure of phragmoplast-nuclei complexes isolated from cultured tobacco cells. *Protoplasma*

(suppl). 2:95–103.
Kakimoto, T., and H. Shiboaka. 1992. Synthesis of polysaccharides in phragmoplasts isolated from tobacco BY-2 cells. *Plant Cell Physiol.* 33:353–361.
Kiss, J. Z., T. H. Giddings, L. A. Staehelin, and F. D. Sack. 1990. Comparison of the ultrastructure of conventionally fixed and high pressure frozen/freeze substituted root tops of *Nicotiana* and *Arabidopsis. Protoplasma.* 157:64–74.
Klausner, R. D., J. G. Donaldson, and J. Lippincott-Schwartz. 1992. Brefeldin A: insights into the control of membrane traffic and organelle structure. *J. Cell Biol.* 116:1071–1080.
Lambert, A.-M. 1993. Microtubule-organizing centers in higher plants. *Curr. Opin. Cell Biol.* 5:116–122.
Mersey, B., and M. E. McCully. 1978. Monitoring the course of fixation of plant cells. *J. Microsc.* 114:49–76.
Moore, P. J., and L. A. Staehelin. 1988. Immunogold localization of the cell wall matrix polysaccharides rhamnogalacturonan I and xyloglucan during cell expansion and cytokinesis in Trifolium pratense L.; implications for secretory pathways. *Planta.* 174:433–445.
Nagata, T., Y. Nemoto, and S. Hasezawa. 1992. Tobacco BY-2 cell line as the "HeLa" cells in the cell biology of higher plants. *Int. Rev. Cytol.* 132:1–30.
Palevitz, B. A. 1980. Comparative effects of phalloidin and cytochalasin B on motility and morphogenesis in Allium. *Can. J. Bot.* 58:773–785.
Pearse, B. M. F., and M. S. Robinson. 1990. Clathrin, adaptors, and sorting. *Annu. Rev. Cell Biol.* 6:151–171.
Platt-Aloia, K. A., and W. W. Thomson. 1982. Freeze-fracture of intact plant tissue. *Stain Technol.* 57:327–334.
Poste, G., and A. C. Allison. 1973. Membrane fusion. *Biochim. Biophys. Acta.* 300:421–465.
Ridge, R. 1988. Freeze substitution improves the ultrastructural preservation of legume root hairs. *Bot. Mag. Tokyo.* 101:427–441.
Roberts, K., and D. H. Northcote. 1970. The structure of sycamore callus cells during division in a partially synchronized suspension culture. *J. Cell Sci.* 6: 299–321.
Schopfer, C. R., and P. K. Hepler. 1991. Distribution of membranes and the cytoskeleton during cell plate formation in pollen mother cells of Tradescantia. *J. Cell Sci.* 100:717–728.
Staehelin, L. A., and R. Chapman. 1987. Secretion and membrane recycling in plant cells: novel intermediary structures visualized in ultrarapidly frozen sycamore and carrot suspension-culture cells. *Planta.* 171:43–57.
Staehelin, L. A., T. G. Giddings, Jr., J. Z. Kiss, and F. D. Sack. 1990. Macromolecular differentiation of Golgi stacks in root tips of Arabidopsis and Nicotiana seedlings as visualized in high pressure frozen and freeze substituted samples. *Protoplasma.* 157:75–91.
Takei, K., P. S. McPherson, S. L. Schmid, and P. DeCamilli .1995. Tubular membrane invaginations coated by dynamin rings are induced by GTP-γS in nerve terminals. *Nature (Lond.).* 374:186–189.
Vantard, M., N. Levilliers, A.-M. Hill, A. Adoutte, and A.-M. Lambert. 1990. Incorporation of *Paramecium* axonemal tubulin into higher plant cells reveals functional sites of microtubule assembly. *Proc. Natl. Acad. Sci. USA.* 87:8825–8829.
Wolniak, S. M, P. K. Hepler, and W. T. Jackson 1980. Detection of the membrane-calcium distribution during mitosis in *Haemanthus* endosperm with chlorotetracycline. *J. Cell Biol.* 87:23–32.
Yasuhara, H., S. Sonobe, and H. Shiboaka. 1993. Effects of taxol on the development of the cell plate and of the phragmoplast in tobacco BY-2 cells. *Plant Cell Physiol.* 34:21–29.
Zhang, D., P. Wadsworth, and P. K. Hepler. 1990. Microtubule dynamics in living dividing plant cells: confocal imaging of microinjected fluorescent brain tubulin. *Proc Natl. Acad. Sci. USA.* 87:8820–8824.
Zhang, D., P. Wadsworth, and P. K. Hepler. 1993. Dynamics of microfilaments are similar, but distinct from microtubules during cytokinesis in living, dividing plant cells. *Cell Motil. Cytoskeleton.* 24:151–155.